Crystal Structure of Isotactic Propylene−Hexene Copolymers: The Trigonal Form of Isotactic Polypropylene

Claudio De Rosa,*,† Stefania Dello Iacono,† Finizia Auriemma,† Eleonora Ciaccia,‡ and Luigi Resconi‡

Dipartimento di Chimica, Università di Napoli "Federico II", Complesso Monte S.Angelo, Via Cintia, I-80126 Napoli, Italy, and Basell Polyolefins, Centro Ricerche Giulio Natta, P.le Donegani 12, I-44100 Ferrara, Italy

Received March 22, 2006; Revised Manuscript Received May 9, 2006

ABSTRACT: A study of the structure of isotactic propylene−hexene random copolymers, prepared with single-center metallocene catalysts, is reported. For low concentrations of hexene comonomeric units, up to nearly 10 mol %, copolymers crystallize in the α form of isotactic polypropylene. Copolymers with hexene contents higher than 10 mol % crystallize in a new polymorphic form that melts at nearly 50 °C. The hexene units are partially included in both crystals of α form and of the new form. The crystallization of the new crystalline form allows incorporation of a high amount of hexene units. The melting temperature and the crystallinity decrease rapidly with increasing hexene content. A slower decrease of melting temperature and crystallinity is observed at high hexene concentrations because of the crystallization of the new form. The crystal structure of the new form has been studied by analysis of X-ray powder and fiber diffraction patterns of samples containing hexene concentration higher than 10 mol %. Chains in 3-fold helical conformation of propylene−hexene copolymers are packed in a trigonal unit cell according to the space group $R3c$ or $R\bar{3}c$. The values of a and b axes of the unit cell depend on hexene concentration, and values of $a = b = 17.5$ Å and $c = 6.5$ Å have been found for the sample with 26 mol % of hexene. The structure contains high degree of disorder due to the constitutional disorder of the random copolymer chains that produces disorder in the positioning of the lateral groups in the unit cell. Moreover, statistical disorder in the up−down positioning of the helical chains and slight disorder in the orientation of chains around the 3-fold axes are present. The inclusion of hexene units in the crystals induces a suitable increase of density that allows crystallization of 3-fold helical chains in the trigonal form, where the helical symmetry of the chains is maintained in the crystal lattice. The structure is similar to that of form I of isotactic polybutene. This form does not crystallize, and has never been observed so far for the polypropylene homopolymer because, in the absence of bulky side groups, it would have a too low density. This structure represents an example of entropy-driven phase formation.

Introduction

The structure and physical properties of isotactic propylene−hexene random copolymers, prepared with metallocene catalysts, of composition variable between 2 and 25 mol % of hexene, have been described in a recent paper.[1] The copolymers are crystalline up to a concentration of hexene as high as 25 mol %. It has been observed that the crystallinity decreases smoothly with increasing hexene content up to about 10 mol %. This observation has suggested that when the concentration of hexene units is less than 10 mol %, the comonomers are excluded from the polypropylene crystals.[1] Copolymers with hexene content higher than 10 mol % crystallize in a new crystalline form, different from the well-known α, β, and γ forms of isotactic polypropylene (iPP) and different from the crystalline form of isotactic poly(1-hexene).[1] Moreover, significant modifications of the crystallization process have been observed. The new crystal structure allows incorporation of hexene units in the crystals. This was inferred from the observed higher level of crystallinity than that would be expected if comonomers were excluded from the crystal and better development of crystals as the hexene content increases.[1]

Copolymers with these high hexene contents crystallize in the new form very slowly. When cooled to ambient temperature from the melt, an incubation period is required before primary nucleation occurs. Long fibrous lamellae, 10−15 nm thick, form around the nucleus. The lamellae rapidly become more numerous as they form sheaflike arrays that develop into small spherulites.[1] From the X-ray diffraction pattern of highly oriented films of the copolymer with 22.4 mol % hexene a preliminary model of the crystal structure of the new form was proposed, consisting in 3-fold helical chains packed in an orthorhombic unit cell with axes $a = 19.86$ A, $b = 17.176$ Å, and $c = 6.458$ Å.[1]

Recently, we have reevaluated the diffraction data and have reported a different preliminary model for this structure, characterized by a smaller trigonal unit cell that houses six 3-fold helices.[2] We have suggested that the driving force that induces the crystallization of this new form is the increase of density due to the inclusion of hexene units in the crystal.[2] The structure of this new form is similar to those of form I of isotactic polybutene and polystyrene and does not crystallize in polypropylene homopolymer because it would have a too low density.[2] It must be mentioned that, parallel to our analysis of this crystal structure, Lotz et al. have reevaluated the original diffraction data of ref 1 and have reached independently a similar conclusion.[3]

In this paper the complete resolution of the crystal structure of the new form that crystallizes in propylene−hexene copolymers is reported. Different types of structural disorder present in the structure are analyzed on the basis of the intensities of

* To whom correspondence should be addressed. Telephone: ++39081 674346. Fax: ++39081 674090. E-mail: claudio.derosa@unina.it.
† Univerisità di Napoli "Federico II", Italy.
‡ Basell Polyolefins, Ferrara, Italy.

10.1021/ma0606354 CCC: $33.50
Published on Web 08/02/2006

Table 1. Compositions (mol % Hexene), Mass Average Molecular Masses ($\bar{M}_w$), Polydispersities ($\bar{M}_w/\bar{M}_n$) and Melting Temperatures (T_m) of Propylene−Hexene Copolymers

sample	mol % hexene	$\bar{M}_w$	$\bar{M}_w/\bar{M}_n$	T_m (°C)
iPPHe1	1.2	699 600	2.3	143
iPPHe2	2.0	122 000	2.4	129
iPHe2.5	2.5	430 800	2.0	127
iPHe3.2	3.2	152 000	2.0	124
iPHe3.7	3.7	333 200	2.0	120
iPPHe4.2	4.2	291 700	2.0	115
iPPHe6.8	6.8	239 500	2.2	99
iPPHe9	9.0	209 800	2.0	93
iPPHe11	11.2	266 300	1.9	65
iPPHe18	18.0	217 400	1.9	49
iPPHe26	26.0	184 500	2.0	50

reflections in the experimental X-ray powder and fiber diffraction patterns and calculation of diffraction patterns of structure models. The role of inclusion of hexene units in the crystals of α form of iPP, at low and high hexene concentrations, and of the crystal density on the crystallization behavior of propylene−hexene copolymers is discussed.

Experimental Section

All analyzed samples of isotactic propylene−hexene copolymers (iPPHe) have been prepared with metallocene catalysts activated with methylaluminoxane. Composition (mol % of hexene comonomeric units), molecular masses, and melting temperatures of all samples are reported in Table 1. The number *N* in the symbol iPPHe*N* indicates the mol % hexene concentration (Table 1). The composition and the chain microstructure were determined by analysis of the ^{13}C NMR spectra. According to this analysis, the copolymers have a random distribution of comonomers ($r_1 \times r_2 \approx 1$). The narrow molecular weight distributions indicate also a homogeneous intermolecular composition.

The melting temperatures were obtained with a differential scanning calorimeter (DSC) Perkin-Elmer DSC-7 performing scans in a flowing N_2 atmosphere and a heating rate of 10 °C/min.

The mass average molecular masses were evaluated from size exclusion cromatography (SEC). The SEC curves of all samples show narrow molecular weight distributions, with $M_w/M_n \approx 2$, typical of single-center metallocene catalysts.

Oriented fibers of the samples iPPHe9, iPPHe11, iPPHe18, and iPPHe26 have been obtained by stretching crystalline compression-molded films at room temperature up to 400−650% deformations. Compression-molded samples have been prepared by heating the powder samples at temperatures higher than the melting temperatures under a press at low pressure, and slowly cooling to room temperature. Copolymer samples containing 18 and 26 mol % of hexene (samples iPPHe18 and iPPHe26) do not crystallize by cooling the melt to room temperature and amorphous films are obtained by compression molding. These amorphous samples slowly crystallize upon aging at room temperature.

X-ray diffraction patterns have been obtained with Ni-filtered Cu Kα radiation. The powder profiles were obtained with an automatic Philips diffractometer, whereas the fiber diffraction patterns were recorded on a BAS-MS imaging plate (FUJIFILM) using a cylindrical camera and processed with a digital imaging reader (FUJIBAS 1800).

The indices of crystallinity (x_c) were evaluated from the X-ray powder diffraction profiles by the ratio between the crystalline diffraction area (A_c) and the total area of the diffraction profile (A_t), $x_c = A_c/A_t$. The crystalline diffraction area has been obtained from the total area of the diffraction profile by subtracting the amorphous halo. The scattering of amorphous phases of samples iPPHe18 and iPPHe26 have been obtained from the X-ray diffraction profiles of the amorphous samples prepared by cooling the melt to room temperature, before crystallization occurs upon aging at room temperature. The amorphous halo of copolymer samples with hexene contents lower that 9 mol %, which crystallize in the α form of iPP, has been obtained from the X-ray diffraction profile of an atactic polypropylene. The scattering of the amorphous phases of samples iPPHe9 and iPPHe11, which crystallize as mixtures of crystals of the α form and the new form, have been obtained by the average of the amorphous haloes of atactic polypropylene and of the sample iPPHe26, weighted with respect to the relative amount of the two crystalline phases. The amorphous scattering was then scaled and subtracted to the X-ray diffraction profiles of the semicrystalline samples.

Densities of the semicrystalline and amorphous copolymer samples were measured by flotation of compression-molded films at 25 °C in solutions of water and ethyl alcohol.

Calculations of packing energy were performed with the software package[4] CERIUS[2], using the force field PCFF.[5]

Calculated structure factors were obtained as $F_c = (\Sigma|F_{hkl}|^2 M_{hkl})^{1/2}$, where F_{hkl} is the structure factor of the *hkl* reflection, M_{hkl} is the multiplicity factor for powder diffraction, and the summation is taken over all reflections included in the 2θ range of the corresponding reflection peak observed in the X-ray powder diffraction profile. A thermal factor $B = 8.9$ Å^2 and the atomic scattering factors as in ref 6 were assumed. The observed structure factors (F_o) were evaluated from the intensities of the reflections observed in the X-ray powder diffraction profile, $F_o = (I_o/LP)^{1/2}$, where *LP* is the Lorentz−polarization factor for X-ray powder diffraction: $LP = (1 + \cos^2 2\theta)/(\mathrm{sen}^2\theta \cos\theta)$. The experimental intensities (I_o) were evaluated by measuring the areas of the peaks in the X-ray powder diffraction profile, after subtraction of the amorphous halo.

Calculated X-ray powder diffraction profiles were obtained with the software package[4] CERIUS[2], using the isotropic thermal factor $B = 8.9$ Å^2 and profile functions having a half-height width regulated by the average crystallite size along *a*, *b*, and *c* axes, $L_a = L_b = L_c = 100$ Å. This value corresponds to a coherence length along *a*, *b*, and *c* and is not a true crystallite size.

The intensities of reflections in the X-ray fiber diffraction pattern were quantitatively compared with calculated square modulus of structure factors. The observed intensities I_o were evaluated by measuring the density of reflection spots recorded on the imaging plate after subtraction of the background intensity. For each reflection the background intensity was determined by measuring the intensity of the region closest to the reflection spot. The observed square modulus of structure factors (F_o^2) were evaluated from the observed intensities, $F_o^2 = I_o/LP$, where *LP* is the Lorentz−polarization factor for fiber diffraction $LP = (1 + \cos^2 2\theta)/[2(\sin^2 2\theta - \zeta^2)^{1/2}]$, with $\zeta = \lambda l/c$, *l* and *c* being the order of the layer line and the chain axis, respectively. The calculated square modulus of structure factors were obtained as $F_c^2 = |F_{hkl}|^2 \cdot M_{hkl}$, where F_{hkl} is the structure factor of the *hkl* reflection and M_{hkl} is the multiplicity factor for fiber diffraction. Simulated X-ray fiber diffraction patterns have been obtained using the software package[4] CERIUS[2], using the isotropic thermal factor $B = 8.9$ Å^2.

Results and Discussion

X-ray Diffraction and Density. The X-ray powder diffraction profiles of as-prepared samples of iPPHe copolymers are reported in Figure 1. It is apparent that the samples crystallize in the α form of iPP up to a concentration of hexene units of nearly 10 mol %, as indicated by the presence of typical 110, 040, and 130 reflections of the α form of iPP at $2\theta = 14$, 17, and 18.6°, respectively, in the diffraction profiles of Figure 1a-f. For a hexene concentration of 9 mol % an additional reflection at $2\theta \approx 10.5°$ appears (Figure 1g) whose intensity increases with increasing hexene content (Figure 1h−l). This indicates that already at 9 mol % of hexene concentration crystals of the new form are obtained in mixture with α form. The copolymer samples with 18 and 26 mol % crystallize totally in the new crystalline form. In fact, for these hexene compositions the X-ray diffraction profiles present reflections at about $2\theta = 10.2$, 17.5, and 20.6° (Figure 1i,l), which do not correspond to reflections typical of crystals of α, *β*, and *γ* forms of iPP. Moreover, as discussed in ref 1, these reflections do not agree with the

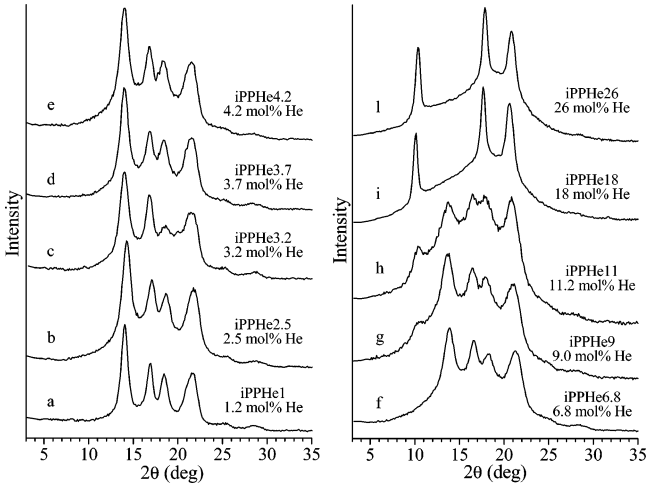

Figure 1. X-ray powder diffraction profiles of as-prepared and aged at room temperature samples of iPPHe copolymers with the indicated concentration of hexene units (He).

reported crystal structures of the different crystalline forms of isotactic poly(1-hexene), described by Turner-Jones,[7] which are, indeed, characterized by a strong reflection at $2\theta = 4°$ that is not observed in the diffraction profiles of Figure 1i,l.

For iPPHe samples with low hexene concentrations that crystallize in the α form of iPP (Figure 1a−h), we have observed that the values of the Bragg distances of 110 and 040 reflections, which occur at $2\theta = 14.2$ and 17.1°, respectively, in the diffraction pattern of α form of iPP homopolymer, slightly increase with increasing hexene concentration (Figure 2A). This indicates an increase of dimensions of *a* and *b* axes of the monoclinic unit cell of α form and inclusion of hexene comonomeric units in crystals of α form. The values of *a* and *b* axes of the unit cell for crystals of α form of iPPHe copolymers are reported in Table 2 and in Figure 2B as a function of hexene content. The values of the chain axis $c = 6.5$ Å and of $\beta = 99.3°$ of the monoclinic unit cell of the α form of iPP[8] have been assumed constant with the hexene content. The unit cell dimensions of α form increase with increasing hexene concentration up to nearly 4−5 mol %, and then achieve constant values for higher hexene contents (Figure 2B), when the new form crystallizes in mixture with the α form.

The hexene units are also included in the crystals of the new polymorphic form at high hexene concentrations. In particular, the change of crystallization habit at hexene contents higher than 10 mol % allows a nearly complete accommodation of hexene units in the crystal lattice. This hypothesis could explain the data of Figure 2, which indicate that crystals of the α form in copolymers with hexene concentrations in the range 4−11 mol % contain nearly the same amount of included hexene units, although the overall hexene concentrations are different. In fact, since for concentrations higher than 9−10 mol % the amount of hexene is such as to induce crystallization of the new form, still in mixture with the α form, most of the hexene units are incorporated in the crystals of the new form, which, therefore, contain an amount of hexene higher than that included in crystals of α form. As a consequence, crystals of α form in the samples iPPHe9 and iPPHe11 include amount of hexene units similar to that in α form crystals of the samples iPPHe3.7 and iPPHe4.2, with similar values of *a* and *b* axes.

The X-ray powder diffraction profiles of some iPPHe samples crystallized from the melt by compression-molding and cooling the melt to room temperature (or below room temperature) at cooling rate of nearly 10 °C/min, are reported in Figure 3.

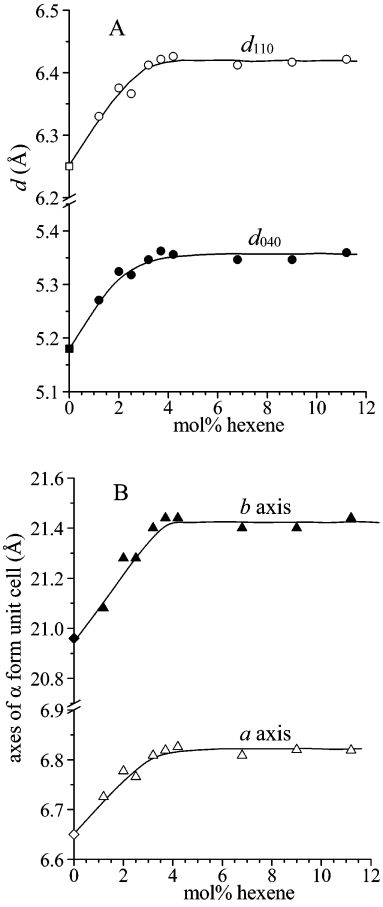

Figure 2. Values of Bragg distances (*d*) of 110 (○) and 040 (●) reflections (A), and of *a* (△) and *b* (▲) axes of the unit cell of the α form (B) that crystallizes in as-prepared samples of iPPHe copolymers as a function of hexene concentration. The values of Bragg distances (□, ■) and *a* and *b* axes (◇, ◆) of the α form of iPP homopolymer are also reported.

Table 2. Values of *a* and *b* Axes of the Monoclinic Unit Cell of the α Form and of the Trigonal Unit Cell of the New Form that Crystallizes in Samples of iPPHe Copolymers[a]

sample	mol % hexene	α form $\beta = 99.3°$, $c = 6.5$ Å *a* (Å)	α form $\beta = 99.3°$, $c = 6.5$ Å *b* (Å)	trigonal form $\gamma = 120°$, $c = 6.5$ Å $a = b$ (Å)
iPP[8]	0	6.65	20.96	
iPPHe1	1.2	6.73	21.08	
iPPHe2	2.0	6.78	21.28	
iPHe2.5	2.5	6.77	21.28	
iPHe3.2	3.2	6.81	21.40	
iPHe3.7	3.7	6.82	21.44	
iPPHe4.2	4.2	6.83	21.44	
iPPHe6.8	6.8	6.81	21.40	
iPPHe9	9.0	6.82	21.40	16.50
iPPHe11	11.2	6.82	21.44	16.65
iPPHe18	18.0			17.15
iPPHe26	26.0			17.50

[a] For samples iPPHe9, iPPHe11, iPPHe18, and iPPHe26 the parameters of the trigonal unit cell of the new form have been obtained from the X-ray fiber diffraction patterns (Figures 8 and 9).

Samples with hexene content up to 11 mol % crystallize from the melt basically in the α form (Figure 3a-e). Samples iPPHe18 and iPPHe26 with 18 and 26 mol % of hexene units, instead, do not crystallize from the melt and amorphous samples are obtained by cooling the melt below room temperature (Figure 3f,g).

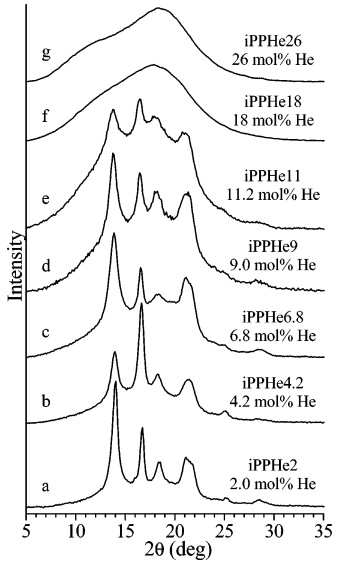

Figure 3. X-ray powder diffraction profiles of samples of iPPHe copolymers with the indicated concentration of hexene units (He), crystallized from the melt by compression-molding and cooling the melt to room temperature (or below room temperature) at nearly 10 °C/min.

Amorphous specimens of the samples iPPHe18 and iPPHe26 slowly crystallize in the new polymorphic form upon aging at room temperature for about 24 h. The X-ray powder diffraction profiles of the samples iPPHe18 and iPPHe26 cooled from the melt to room temperature and aged at room temperature for different times are reported in Figure 4, parts A and B. The degree of crystallinity of both samples is reported in Figure 4C as a function of the aging time. It is apparent that almost complete crystallization of the new form occurs for both samples in about 24 h. The slow crystallization rate at room temperature is probably related to the low melting temperature (50 °C, Table 1) and the consequent low undercooling at room temperature.

The fact that the new form does not crystallize from the melt by cooling explains the experimental observation that the samples iPPHe9 and iPPHe11, which were crystallized as a mixture of α form and the new form in the as-prepared and aged samples (Figure 1g,h), crystallize from the melt only in the α form. In fact, the reflection at $2\theta = 10.2°$ of the new form is absent in the diffraction profiles of Figure 3d,e.

All iPPHe copolymer samples with hexene content up to 11.2 mol % exhibit a crystallization exotherm in the DSC cooling curves from the melt, recorded at 10 °C/min, due to the crystallization of the α form. The crystallization temperature decreases with increasing hexene content, up to −1 °C for the sample iPPHe11. The DSC cooling and heating curves, recorded at scanning rate of 10 °C/min, of samples iPPHe18 and iPPHe26 that do not crystallize from the melt, are reported in Figure 5. The DSC curves corresponding to the cooling of the melt below room temperature (curves a of Figure 5) and the subsequent heating (curves b of Figure 5), exhibit only change of heat capacity indicating a glass transition temperature in the range between −10 and −20 °C. The DSC heating curves of the samples aged at room temperature for two months, recorded at heating rate of 10 °C/min, indicate melting temperature of the new form of nearly 50 °C (curves c of Figure 5). As-prepared samples, aged at room temperature, show DSC heating thermograms similar to the curves c of Figure 5.

The melting temperatures and the degree of crystallinity of as-prepared samples (and aged at room temperature for long time) and melt-crystallized samples of the copolymers iPPHe are reported in Figure 6A and B, respectively. The melting temperatures of melt-crystallized samples correspond to those of samples obtained by cooling the melt to room temperature (or below room temperature) at cooling rate of 10 °C/min. The degrees of crystallinity of as-prepared samples have been evaluated from the X-ray powder diffraction profiles of Figure 1, whereas the degrees of crystallinity of melt-crystallized samples correspond to those of compression-molded samples without aging at room temperature (as the samples of Figure 3). Only for the samples iPPHe18 and iPPHe26, which are amorphous soon after the compression molding (Figures 3 and 4), does the crystallinity correspond to compression-molded samples after complete crystallization by aging at room temperature for 2 months.

The decrease of melting temperature and crystallinity with increasing hexene content is fast up to 7−8 mol % and then

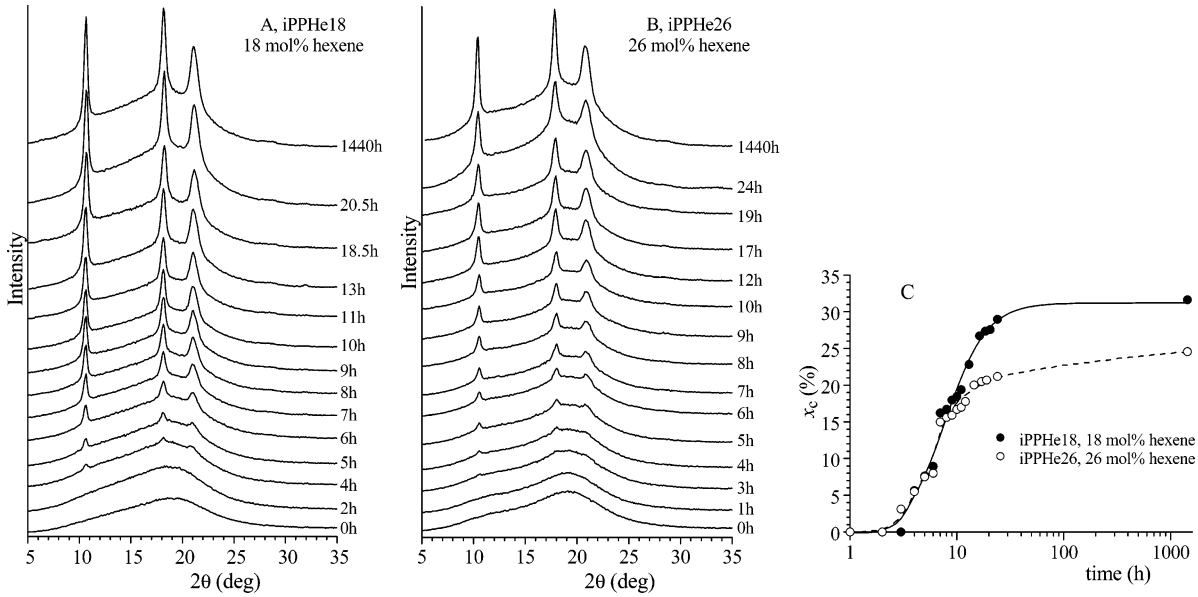

Figure 4. X-ray powder diffraction profiles of the samples iPPHe18 (A) and iPPHe26 (B) with 18 and 26 mol % of hexene units, respectively, cooled from the melt to room temperature and aged at room temperature for the indicated aging time. (C) Degree of crystallinity for samples iPPHe18 (●) and iPPHe26 (○) as a function of the aging time at room temperature.

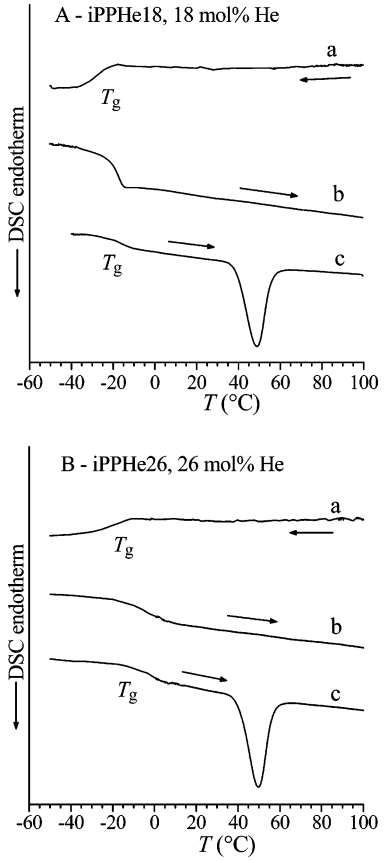

Figure 5. DSC curves of samples iPPHe18 with 18 mol % of hexene (A) and iPPHe26 with 26 mol % of hexene (B) recorded at scanning rate of 10 °C/min. The cooling curves from the melt (a), the subsequent heating curves (b) and the heating curves of the samples cooled from the melt and aged at room temperature for two months (c) are shown.

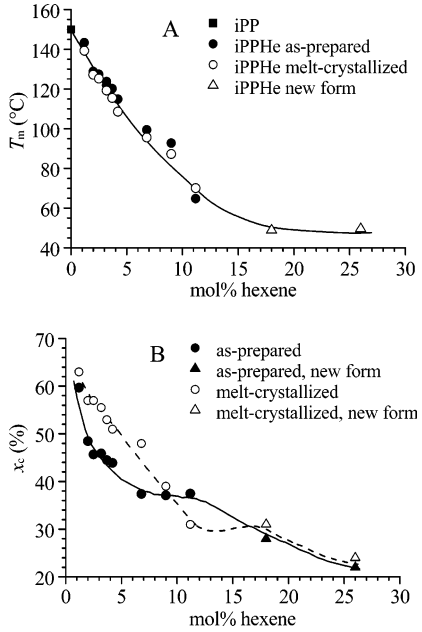

Figure 6. Melting temperature (A) and crystallinity (B) of as-prepared (●, ▲) and melt-crystallized (○, △) samples of iPPHe copolymers crystallized in the α form of iPP (●, ○) and in the new form (▲, △), as a function of hexene concentration. The melting temperature of the iPP homopolymer sample prepared with the same catalyst is also reported (■). In part A, the melting temperatures of melt-crystallized samples correspond to those of samples obtained by cooling the melt to room temperature (or below room temperature) at cooling rate of 10 °C/min. In part B, the crystallinity of melt-crystallized samples corresponds to that of compression-molded samples. Only for the samples iPPHe18 and iPPHe26 with 18 and 26 mol % of hexene, which are amorphous soon after the compression molding, the crystallinity corresponds to that of compression-molded samples after crystallization at room temperature for 2 months (△).

becomes slower for higher hexene concentrations (Figure 6). This is in agreement with the hypothesis that hexene units are included in the crystals of α form for low concentrations and act as a lattice defect, producing large disturbance of the crystalline lattice and a consequent decrease of melting temperature, melting enthalpy and crystallinity. For concentrations higher than 7−8 mol %, larger amounts of hexene units are more easily accommodated in the crystalline lattice of the new form, producing a lower decrease of crystallinity and melting temperature. The crystallinity is, indeed, nearly constant for as-prepared and aged samples with hexene concentration in the range 7−13 mol % (Figure 6B). It is also worth noting from Figure 6B that the crystallinity of melt-crystallized samples is generally higher than that of as-prepared samples. Only for samples having hexene content in the range 10−15 mol % the crystallinity of melt-crystallized specimens is lower than that of as-prepared and aged samples. This is due to the absence of the additional contribution of crystallinity of the new form in the melt-crystallized and not aged samples.

The inclusion of hexene comonomeric units in the crystals has been confirmed by measurements of the density of the crystalline phase of the iPPHe copolymers. The values of the experimental density of the semicrystalline iPPHe samples, measured by flotation on compression-molded films aged at room temperature, are reported in Figure 7A. For samples iPPHe11 and iPPHe26 the compression-molded films have been aged at room temperature for 30 h and 12 h, respectively, so that the measurement of density has been performed on samples having crystallinity of 31% and 17%, respectively (Figure 4C). The density decreases with increasing hexene concentration, according to the decrease of crystallinity (Figure 6B). A slower decrease is observed for hexene concentrations higher than 10 mol %, when the new form crystallizes.

The values of density of the crystalline phase of copolymers iPPHe are reported in Figure 7B. These values have been evaluated from the experimental density of Figure 7A, the crystallinity of Figures 6B and 4C and the density of amorphous phases. The value $\rho_a = 0.854$ g/cm^3 of the density of amorphous iPP[9] has been assumed for the density of amorphous phases of iPPHe samples with hexene contents up to 11.2 mol %. The values of densities of amorphous phases of samples iPPHe18 and iPPHe26, $\rho_a = 0.852$ and 0.849 g/cm^3, respectively, have been instead measured by flotation on the compression-molded amorphous samples, before they crystallize by aging at room temperature.

For copolymers with hexene content up to nearly 10 mol % that crystallize in the α form of iPP, the experimental density of α form crystals decreases with increasing hexene concentration (Figure 7B). This indicates that for this range of hexene content the expansion of unit cell volume, due to inclusion of hexene units, is not compensated by increase of mass because hexene units are, probably, not completely included in the crystals of α form. This is confirmed in Figure 7B by comparing the experimental crystalline density with the theoretical density of α form crystals, calculated assuming complete inclusion of hexene units in the crystals and values of unit cell volume calculated from the experimental values of axes of unit cells of Table 2. It is apparent that for samples with hexene contents up to 11 mol %, the values of the calculated crystalline density are much higher than the experimental ones, indicating that for

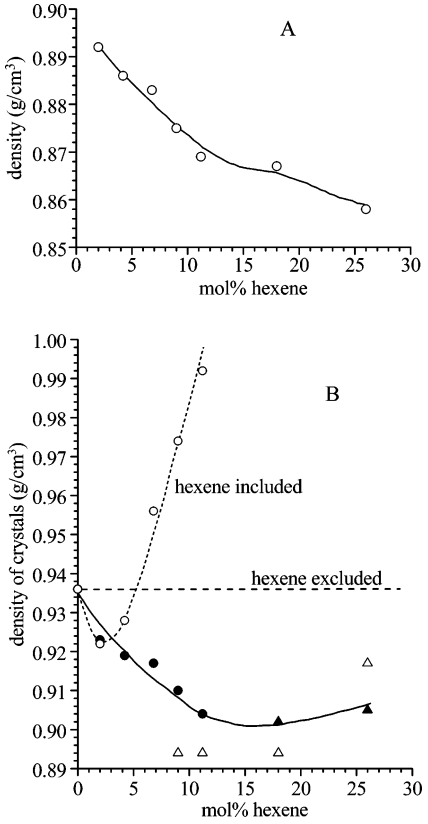

Figure 7. Values of experimental density (A) and of density of the crystalline phase (B) of samples of copolymers iPPHe, as a function of hexene concentration. In B the experimental densities of crystals of α form (●) and of the new form (▲) of copolymers iPPHe are compared with the theoretical densities of crystals of α form (○) and of the new form (△) calculated assuming complete inclusion of hexene units in the crystals and a volume of the unit cell calculated from the experimental values of the unit cell parameters reported in Table 2. The condition of complete exclusion of hexene units from the crystals of α form is shown as the dashed line (the density of crystals is constant at the value of iPP, $\rho_c = 0.936$ g/cm^3). For samples iPPHe9 and iPPHe11 with 9.0 and 11.2 mol % of hexene, the experimental values of the crystalline density (●) refer only to crystals of the α form because the trigonal form has been obtained only in fiber samples and only the values of the calculated density of the trigonal crystals are reported (△).

these samples the hexene units are only in part included in the crystals of α form. Only for low hexene content, up to 2 mol %, the calculated and experimental crystalline densities are similar indicating nearly complete inclusion of hexene in the crystals of α form (Figure 7B).

For iPPHe samples with hexene contents higher than 10 mol % that crystallize in the new form, the values of theoretical density of crystals of the new form, calculated from the experimental values of axes of the trigonal unit cell of Table 2 and assuming complete inclusion of hexene units in the crystals of the new form, are very similar to the experimental values of crystalline density. This indicates that the crystallization of the new form allows much higher incorporation of hexene units in the crystals and a density of crystals as high as 0.91 g/cm^3 is achieved for the highest hexene concentration.

Oriented Fibers of the New Form. Oriented fibers of the samples iPPHe9, iPPHe11, iPPHe18, and iPPHe26 have been obtained by stretching at room-temperature compression-molded films up to 400−650% deformations. Since the compression-molded films of samples iPPHe18 and iPPHe26 are amorphous (Figure 3f,g) but crystallize at room temperature into the new form (Figure 4), the stretching has been performed after the complete crystallization of the films (Figure 4). Compression-molded films of the samples iPPHe9 and iPPHe11 are instead crystallized into α form of iPP (Figure 3d,e).

The X-ray fiber diffraction patterns of fibers of the samples iPPHe26 and iPPHe18 stretched at 650 and 400% deformations, respectively, and annealed at 50 °C for 20 min, are reported in Figure 8A and B, respectively. The corresponding diffraction profiles read along the equatorial layer lines are reported in Figure 9 (profiles a and b, respectively). Similar patterns are obtained for the ununnealed fibers. Both diffraction patterns of Figure 8, parts A and B, show similar reflections on the equator and first layer line, the only difference being the exact values of the 2θ angles of the most intense reflections. The pattern of the sample iPPHe26 of Figure 8A shows reflections at $2\theta =$ 10.15, 17.5, and 20.3° on the equator (profile a of Figure 9), as observed in the powder diffraction profile (Figure 1l and 4B), and a strong reflection at $2\theta = 20.6°$ on the first layer line. Slightly higher values of the Bragg angles, at $2\theta = 10.3$, 17.6 and 20.4° on the equator and at $2\theta = 20.8°$ on the first layer line are observed in the diffraction pattern of the sample iPPHe18 (Figure 8B and profile b of Figure 9). This indicates slightly different dimensions of the unit cells of the new form for the two samples depending on the hexene concentration.

It is worth noting that a similar X-ray fiber diffraction pattern has been reported by Poon et al.[1] for a copolymer sample containing 25 mol % of hexene.

The reflections observed in the X-ray diffraction pattern of Figure 8A for the sample iPPHe26 with the highest concentration of hexene are listed in Table 3 in comparison with reflections observed in the powder diffraction profile of Figure 1l. From the fiber patterns a chain axis periodicity $c = 6.5$ Å has been evaluated. This indicates that in this new crystalline form the chains keep the stable 3_1 helical conformation typical of the α, β, and γ forms of iPP.

All the reflections observed in the powder and fiber diffraction patterns of the sample iPPHe26 are accounted for by a hexagonal, or trigonal, unit cell with axes $a = b = 17.5$ Å and $c = 6.5$ Å. The unit cell houses six chains of copolymer iPPHe in 3-fold helical conformation. As discussed above, assuming that in the sample iPPHe26 the hexene comonomeric units are included in the crystals, the theoretical density of crystals of the new form is $\rho_{cr} = 0.917$ g/cm^3 for six chains in the unit cell (Figure 7B). This is in agreement with the experimental density $\rho = 0.86$ g/cm^3 of the sample iPPHe26 having a crystallinity of 17% (Figure 7A) and with the experimental density of the crystalline phase $\rho_{cr} = 0.905$ g/cm^3 (Figure 7B).

In the case of the sample iPPHe18 the positions of reflections in the diffraction pattern of Figure 8B (profile b of Figure 9) indicate a slightly smaller hexagonal (trigonal) unit cell with axes $a = b = 17.15$ Å and $c = 6.5$ Å, due to the smaller amount of hexene units included in the unit cell than that of the sample iPPHe26. Assuming these values of unit cell parameters and complete inclusion of hexene units (18 mol %) in the crystals of the sample iPPHe18 (Figure 7), the theoretical density of crystals of the new form is $\rho_{cr} = 0.894$ g/cm^3 for six chains in the unit cell. This is in agreement with the experimental density $\rho = 0.867$ g/cm^3 of the sample iPPHe18 having a crystallinity of 31% (Figure 7A) and with the experimental density of the crystalline phase $\rho_{cr} = 0.902$ g/cm^3 (Figure 7B).

The X-ray fiber diffraction patterns of fibers of the samples iPPHe11 and iPPHe9 with 11.2 and 9.0 mol % of hexene, respectively, are reported in Figure 8, parts C and E, respectively. The corresponding diffraction profiles read along the

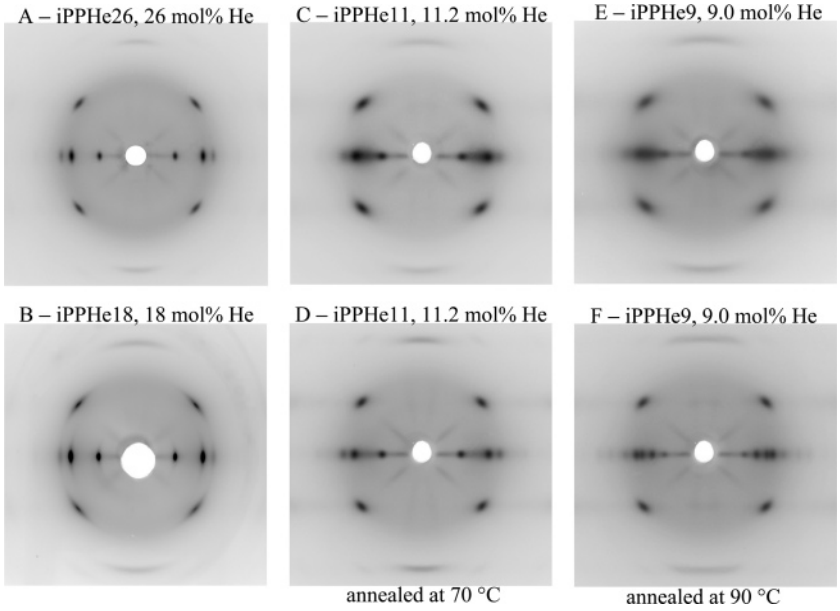

Figure 8. X-ray fiber diffraction patterns of oriented fibers of copolymer samples iPPHe26 annealed at 50 °C (A), iPPHe18 annealed at 50 °C (B), iPPHe11 (C), iPPHe11 annealed at 70 °C (D), iPPHe9 (E), and iPPHe9 annealed at 90 °C (F).

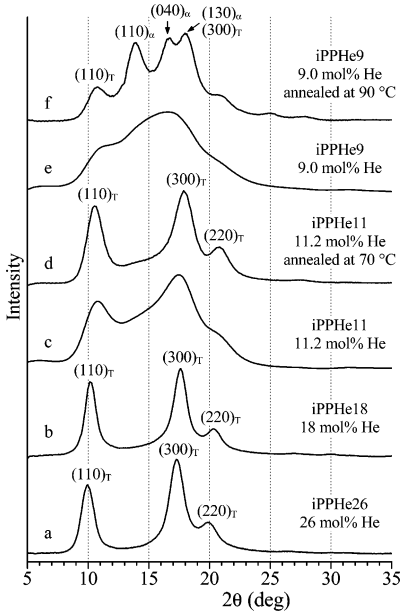

Figure 9. X-ray diffraction profiles read along the equatorial layer lines of the fiber diffraction patterns of Figure 8 of oriented fibers of copolymer samples iPPHe26 (a), iPPHe18 (b), iPPHe11 (c), iPPHe11 annealed at 70 °C (d), iPPHe9 (e), and iPPHe9 annealed at 90 °C (f). The $(110)_T$, $(300)_T$, and $(220)_T$ reflections of the trigonal form and the $(110)_\alpha$, $(040)_\alpha$, and $(130)_\alpha$ reflections of the α form are indicated.

equatorial layer lines are reported in Figure 9 (profiles c and e, respectively). Contrary to samples iPPHe18 and iPPHe26, whose compression-molded films (aged at room temperature) present crystals of the new form (Figure 4), which are oriented by stretching (Figure 8A,B), compression-molded films of the samples iPPHe9 and iPPHe11 are in the common α form of iPP (Figure 3d,e). Crystals of α form, present in the initial compression-molded film (Figure 3d,e), transform by stretching into the new trigonal form, as indicated by the presence of broad equatorial reflections at $2\theta \approx 10$ and 17° in the diffraction patterns of Figure 8, parts C and E (profiles c, e of Figure 9). The clear presence of an additional diffuse halo on the equator in the range $2\theta = 14-18°$, centered at a value of 2θ of nearly 16°, along with the broad intensity maxima at $2\theta \approx 10$ and 17°

Table 3. Experimental Diffraction Angles (2θ), Bragg Distances (d_o) and Intensities of Reflections Observed in the X-ray Powder and Fiber Diffraction Patterns of the Sample iPPHe26 with 26 Mol % of Hexene of Figures 8A and 1l[a]

X-ray fiber diffraction pattern				X-ray powder diffraction profile			
hkl	2θ (deg)	d_o (Å)	*I*	*hkl*	2θ (deg)	d_o (Å)	*I*
110	10.15	8.71	210	110	10.15	8.71	545
300	17.53	5.05	510	300	17.55	5.05	530
220	20.30	4.37	91	220 + 211	20.60	4.31	570
410	26.73	3.34	16				
330	30.83	2.90	3				
600	35.43	2.53	2				
211	20.60	4.31	299				
321	29.59	3.02	10				
511	35.83	2.51	4				
43$\bar{1}$	38.59	2.33	3				
10$\bar{2}$	27.97	3.19	n.e.[b]	10$\bar{2}$	28.25	3.16	45
21$\bar{2}$	31.51	2.84	9				
502	40.34	2.24	4				

[a] The Miller indices *hkl* of reflections, based on the trigonal unit cell with axes $a = b = 17.5$ Å and $c = 6.5$ Å, are also reported. [b] The intensity of the nearly meridional reflection has not been evaluated (n.e.).

(Figure 8C,E and profiles c and e of Figure 9), especially for the sample iPPHe9 (Figure 8E and profile e of Figure 9), indicates that crystals of the α form transform in part into the mesomorphic form of iPP and in part into the new trigonal form. The transformation of α or γ forms of iPP into the mesomorphic form by stretching of metallocene-made iPP samples at high deformations has been extensively discussed in the recent literature.[10,11] The result obtained here, that the α form transforms into the new trigonal form by stretching of propylene−hexene copolymer samples with relatively low hexene concentration (Figure 8, parts C and E), is instead quite unexpected.

The broadness of reflections in the patterns of Figure 8, parts C and E (profiles c and e of Figure 9), indicates that small and, probably highly disordered, crystals of the trigonal form are obtained for the samples iPPHe11 and iPPHe9. To check the stability of the new trigonal form with respect to the α form in the stretched fibers of these samples, the fibers of Figure 8C,E have been annealed for 20 min at temperatures close or slightly above the melting temperatures of the unoriented samples (90 and 70 °C for the samples iPPHe9 and iPPHe11, respectively),

keeping the fiber under tension. The X-ray fiber diffraction patters of annealed fibers of samples iPPHe11 and iPPHe9 are reported in Figure 8, parts D and F, respectively. The corresponding diffraction profiles read along the equatorial layer lines are reported in Figure 9 (profiles d and f, respectively). It is apparent the presence of well-resolved and much sharper equatorial reflections of the trigonal form at $2\theta \approx 10$ and 17°, indicating improvement of crystals of the trigonal form by annealing. In the case of the sample iPPHe9, annealing also produces, as expected, transformation of the mesomorphic form into α form of iPP, as indicated by the presence of reflections at $2\theta = 13.9$, 16.7, and 18.2°, corresponding to the 110, 040, and 130 reflections of the α form, in the diffraction pattern of Figure 8F (see equatorial profile f of Figure 9). The annealed fiber of the sample iPPHe9 is therefore crystallized as a mixture of the new trigonal form and of the α form with a higher amount of α form. Surprisingly, in the case of the sample iPPHe11, the mesomorphic form of iPP transforms by annealing completely into the new trigonal form, rather than into the α form, as indicated by the disappearance of the diffuse equatorial halo in the 2θ range between 14 and 18° in the diffraction pattern of Figure 8D (profile d of Figure 9) and the presence of only reflections of the trigonal form. The data of Figure 8, parts C and D, indicate that, even though the copolymer sample iPPHe11 crystallizes from the melt only in the α form of iPP (Figure 3e), the new trigonal form is more stable than the α form in stretched fibers, because of the presence of hexene comonomeric units.

The positions of reflections of the trigonal form observed in the X-ray fiber diffraction patterns of the annealed fibers of the samples iPPHe11 and iPPHe9 of Figure 8, parts D and F, respectively, are at values of 2θ higher than those observed for the samples iPPHe26 and iPPHe18 (Figure 8A,B). A clear shift toward higher values of 2θ of the reflections at $2\theta \approx 10$ and 17° is, indeed, observed in the profiles of Figure 9 with decreasing hexene concentration. The equatorial reflections are, indeed, at $2\theta = 10.63$, 17.98, and 21.03°, and the first layer line reflection is at $2\theta = 21.05°$ in the diffraction pattern of the sample iPPHe11 (Figure 8D, profile d of Figure 9). In the case of the sample iPPHe9, instead, the reflections of the trigonal form in the diffraction pattern of the annealed fiber of Figure 8F are observed at $2\theta = 10.73°$, 18.2° (superimposed to the 130 reflection of the α form) and 21.07° on the equator (profile f of Figure 9) and at $2\theta = 21.24°$ on the first layer line. According to these values of the Bragg angles, the axes of the trigonal unit cells are smaller than those of samples iPPHe26 and iPPHe18 due to the smaller amount of hexene units (9 and 11.2 mol %) included the unit cell, and precisely $a = b = 16.65$ Å and $c = 6.5$ Å for the sample iPPHe11, and $a = b = 16.50$ Å and $c = 6.5$ Å for the sample iPPHe9 with 9.0 mol % of hexene. Assuming these values of unit cell parameters and complete inclusion of hexene units (9 and 11.2 mol %) in the crystals of the samples iPPHe9 and iPPHe11, the theoretical density of crystals of the new form is, for both samples, $\rho_{cr} = 0.894$ g/cm^3 for six chains in the unit cell, similar to that of the sample iPPHe18. These data confirm that, as observed for crystals of α form (Figure 2B), the dimensions of axes of the trigonal unit cell of the new form depend on the hexene concentration. The values of axes of the trigonal unit cell are reported in Table 2. The values of *a* and *b* axes of the trigonal unit cell increase with increasing hexene concentration.

It is worth noting that the lattice expansion is not necessarily a reflection of inclusion of comonomeric units in the crystals, but it may also be caused by strains at interface of thin crystallites related to the segregation of bulky comonomers in this region, as demonstrated for instance for copolymers of polyethylene with various comonomers.[12] However, in the case of iPPHe copolymers, the density arguments (Figure 7) and the trends of melting temperature and crystallinity (Figure 6) support the hypothesis of inclusion.

Crystal Structure of the Trigonal Form. To give a model of packing of the new form and resolve the crystal structure we refer only to the diffraction data of Table 3 of the sample iPPHe26 with 26 mol % of hexene and the corresponding parameters of the unit cell $a = b = 17.5$ Å and $c = 6.5$ Å. According to this hexagonal unit cell, the four most intense reflections at $2\theta = 10.15$, 17.5, 20.3, and 20.6° are indexed with Miller indices 110, 300, 220, and 211 (Table 3). This suggests that the 3/1 helical chains are packed in a trigonal lattice with a rhombohedral symmetry according to the space group *R*3*c*. The unit cell and the mode of packing are therefore very similar to those in the crystal structures of most of isotactic polyolefins having chains in 3-fold helical conformation, that is, form I of isotactic poly(1-butene) (iPB),[13] polystyrene,[14] poly(vinyl methyl ether),[15] poly(*o*-fluorostyrene),[16] and 1,2-poly(1,3-butadiene).[17] The X-ray powder and fiber diffraction patterns of the new form (Figures 1i,l and 8) are, indeed, very similar to those of form I of iPB.[13]

A model of the crystal structure of the new trigonal form, according to the space group *R*3*c*, is shown in Figure 10. The 3_1 helical symmetry of the chains is maintained in the lattice and the chain axes coincide with the crystallographic 3-fold axes. The structure contains high degree of disorder due to the constitutional disorder of the random copolymer chains that produces disorder in the positioning of the lateral groups in the unit cell. The orientation of the chains around the 3-fold axes have been found by packing energy calculations and from the best agreement between calculated and experimental diffraction patterns. Because of the disorder in the positioning of hexene units inside the unit cell, a disorder in the orientation of chains around the chain axes may also be present. In fact, each chain containing 26 mol % of hexene units randomly distributed along the chain bears on average one hexene unit in a turn of the helix included in the chain axis (as in the model of Figure 10). Therefore, the lowest energy packing is probably achieved for slightly different orientations of the six chains included in the unit cell. A good agreement between calculated structure factors and experimental intensities of reflections observed in powder and fiber diffraction patterns has been obtained introducing slight rotational disorder, corresponding to rotations of the chains of about ±17° around the chain axes with respect to the average positions of chains shown in the model of Figure 10. A comparison between observed and calculated structure factors for the model of Figure 10 in the space group *R*3*c* and for a disordered model characterized by slight disorder in the orientation of chains around the chain axes is reported in Tables 4 and 5 for powder and fiber diffraction patterns, respectively.

It is apparent that the agreement is improved by introducing the rotational disorder. In fact, the intensity of the 300, 330, 600, $31\bar{1}$, and 511 reflections decreases and those of 110 and 220 reflections increase for the disordered model according to the experimental intensities observed in the X-ray powder and fiber diffraction patterns (Tables 4 and 5). However, the calculated intensities of 211, $31\bar{1}$, 321, 511, and 202 reflections are still too high compared to the observed intensities (Tables 4 and 5). A better agreement has been obtained by introducing another type of disorder in addition to the rotational disorder, that is the disorder in the up/down position of the chains. This

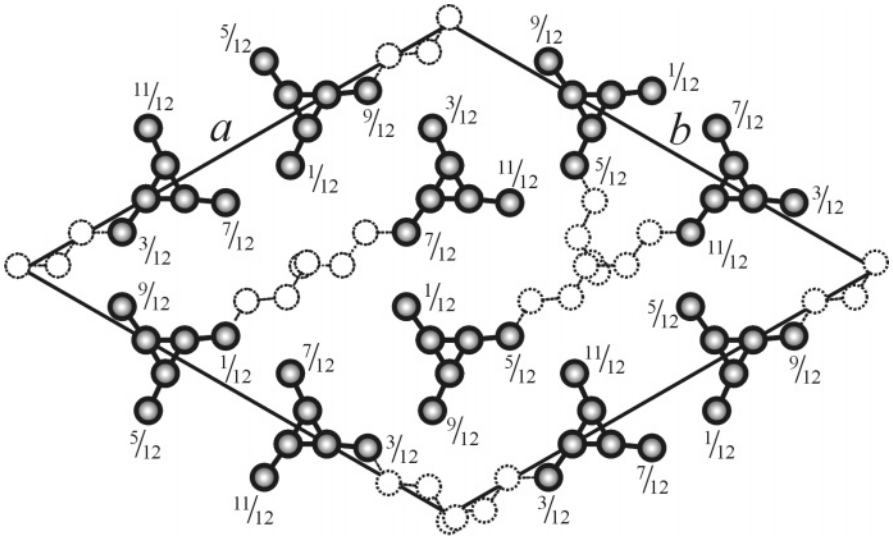

Figure 10. Model of the crystal structure of the trigonal form of iPP in the space group *R*3*c* found in propylene−hexene copolymers. The atoms of propyl side groups of the hexene comonomeric units, randomly distributed along each iPP chain, are shown as thin dotted lines. The *z* fractional coordinates of the methyl carbon atoms are reported in *c*/12 unit.

Table 4. Comparison between Observed Structure Factors (F_o), Evaluated from the Intensities Observed in the X-ray Powder Diffraction Profile of the Sample iPPHe26 of Figure 1l, and Calculated Structure Factors (F_c) for the Model of Packing of the Trigonal Form of Figure 10, in the Space Group *R*3*c*, for the Model of Figure 10 (Space Group *R*3*c*) Containing Disorder in the Orientation of Chains around the Chain Axes (Slight Rotation of about ±17° with Respect to the Model of Figure 10) and for the Limit Disordered Model of Figure 11 in the Space Group *R*3̄*c*[a]

						$F_c = (\Sigma\|F_i\|^2 M_i)^{1/2}$		
hkl	$2\theta_o$ (deg)	$2\theta_c$ (deg)	d_o(Å)	d_c(Å)	F_o	*R*3*c*	*R*3*c* (rot. disorder)	*R*3̄*c* (rot. and up/down disorder)
110	10.15	10.11	8.71	8.750	174	136	183	183
300	17.55	17.55	5.05	5.052	300	393	327	316
220	20.6	20.30	4.31	4.375	366	144 } 351	171 } 335	171 } 281
21$\bar{1}$		20.67		4.297		320 }	288 }	224 }
31$\bar{1}$		25.23		3.530		139	125	32
41$\bar{0}$		26.96		3.307		89	43	4
10$\bar{2}$	28.2	28.08	3.16	3.178	143	148	139	135
321		29.13		3.066		69	99	64
202		29.91		2.987		87	74	4
33$\bar{0}$		30.65		2.917		76	54	54
21$\bar{2}$		31.65		2.827		27	46	43
42$\bar{1}$		34.21		2.621		43	66	40
312		34.90		2.571		55	11	2
600		35.54		2.526		89	50	40
51$\bar{1}$		35.76		2.511		254	193	15
40$\bar{2}$		36.42		2.468		43	28	24
52$\bar{0}$		37.04		2.427		75	72	69
32$\bar{2}$		37.89		2.374		46	28	27
431		38.70		2.326		23	16	14
502		40.70		2.217		69	56	46

[a] The Bragg angles ($2\theta_o$) and the Bragg distances (d_o) of reflections observed in the X-ray powder diffraction profile of the sample iPPHe26 of Figure 1l, and those calculated ($2\theta_c$ and d_c) for the trigonal unit cell with axes $a = b = 17.5$ Å and $c = 6.5$ Å are reported.

means that in each site of the lattice up or down chains, having the same chirality, can be found with the same probability. A limit disordered model, containing statistical up−down disorder, that can be described by the statistical space group *R*3̄*c*, is shown in Figure 11. This type of disorder is also present in the structure of form I of iPB.[13] A comparison between observed and calculated structure factors for the limit disordered model of Figure 11 in the space group *R*3̄*c* is reported in Tables 4 and 5. It is apparent that the intensities of 211, 31$\bar{1}$, 321, 511, and 202 reflections decrease for the model of Figure 11 and a fairly good agreement is obtained.

A direct comparison between the experimental X-ray powder diffraction profile of the new form, after the subtraction of the amorphous halo, obtained for the sample iPPHe26, and the diffraction profile calculated for the model of structure of Figure 10 in the space group *R*3*c* containing disorder in the orientation of the chains around the chain axes, and for the limit disordered model of Figure 11 in the space group *R*3̄*c*, containing statistical up−down disorder, is shown in Figure 12A. The bidimensional X-ray fiber diffraction patterns calculated for the models of Figures 10 and 11, to be compared with the experimental fiber diffraction pattern of Figure 8A, are also reported in Figure 12, parts B and C, respectively. It is apparent that a fairly good agreement has been obtained for the disordered model of Figure 11.

These data indicate that the structure presents disorder in the orientation of chains around the chain axes and up−down disorder, along with the constitutional disorder. Moreover, disorder in the conformation of the lateral groups, in particular for the possible presence of bonds in gauche conformation, may also be present. The real structure is probably intermediate between the limit disordered model *R*3̄*c* of Figure 11 and the

Table 5. Comparison between Observed Structure Factors (F_o), Evaluated from the Intensities Observed in the X-ray Fiber Diffraction Pattern of the Sample iPPHe26 with 26 mol % of Hexene of Figure 8A, and Calculated Square Modulus of Structure Factors (F_c^2) for the Model of Packing of the Trigonal Form of Figure 10, in the Space Group *R*3*c*, for the Model of Figure 10 (Space Group *R*3*c*) Containing Disorder in the Orientation of Chains around the Chain Axes (Slight Rotation of about ±17° with Respect to the Model of Figure 10) and for the Limit Disordered Model of Figure 11 in the Space Group $R\bar{3}c$[a]

						$F_c^2 = \lvert F_{hkl}\rvert^2 M_{hkl}$		
hkl	$2\theta_o$ (deg)	$2\theta_c$ (deg)	d_o (Å)	d_c (Å)	F_o^2	*R*3*c*	*R*3*c* (rot. disorder)	$R\bar{3}c$ (rot. and up/down disorder)
110	10.15	10.11	8.71	8.750	129	93	167	167
300	17.53	17.55	5.06	5.052	554	771	535	500
220	20.30	20.30	4.37	4.375	116	103	146	146
410	26.73	26.96	3.34	3.307	27	39	9	
330	30.83	30.65	2.90	2.917	5	29	15	15
600	35.43	35.54	2.53	2.526	4	40	12	8
520		37.04		2.427		28	26	24
440		41.27		2.187		6	4	4
211	20.61	20.67	4.31	4.297	123	256	207	125
311		25.23		3.530		48	39	3
321	29.59	29.13	3.02	3.066	7	12	25	10
421		34.21		2.621		5	11	4
511	35.83	35.76	2.51	2.511	3	162	94	1
431	38.59	38.70	2.33	2.326	3	1	1	1
102	27.97	28.08	3.19	3.178	n.e.[b]	110	96	91
202		29.91		2.987		38	28	
212	31.51	31.65	2.84	2.827	9	2	5	5
312		34.89		2.571		8		
402		36.42		2.467		9	4	3
322		37.89		2.374		5	2	2
502	40.34	40.70	2.24	2.217	6	24	16	11
512		43.36		2.087		3	1	1

[a] The Bragg angles ($2\theta_o$) and the Bragg distances (d_o) of reflections observed in the X-ray fiber diffraction pattern of the sample iPPHe26 of Figure 8A, and those calculated ($2\theta_c$ and d_c) for the trigonal unit cell with axes $a = b = 17.5$ Å and $c = 6.5$ Å are reported. [b] The intensity of the nearly meridional reflection has not been evaluated (n.e.).

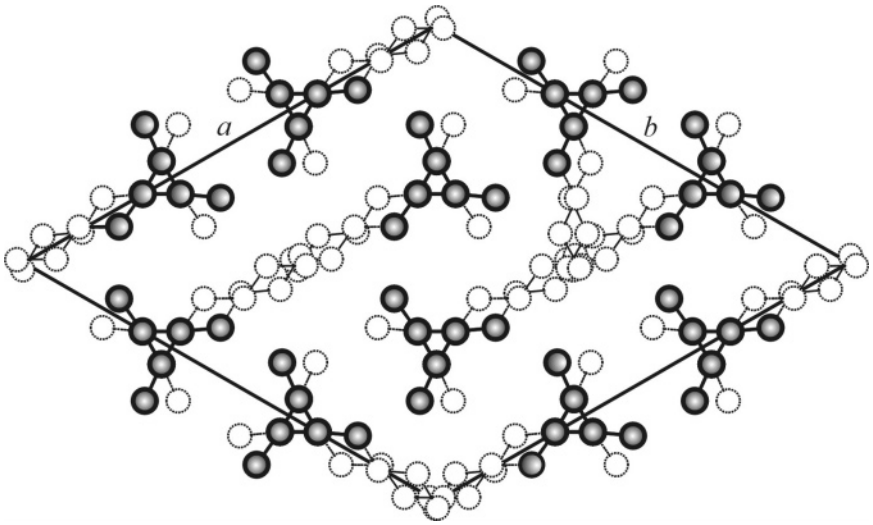

Figure 11. Limit disordered model of the crystal structure of the trigonal form of iPP in the statistical space group $R\bar{3}c$ found in propylene−hexene copolymers. The structure presents statistical disorder in the positioning of up and down chains in each site of the lattice. Two anticlined chains (up and down) having the same chirality that occupy the same lattice site are indicated with thick and thin-dotted lines. The atoms of propyl side groups of the hexene comonomeric units, randomly distributed along each iPP chain, are shown as thin dotted lines.

model *R*3*c* of Figure 10 containing rotational disorder, with a non complete statistical up−down disorder. This is indicated by the presence of some reflections, as for instance the 410 reflection at $2\theta = 26.7°$, which are calculated with too low intensity for the model of Figure 11 (Table 5). This is also evident in Figure 12A where the experimental intensity of the peak corresponding to 211 + 220 reflections (curve a) is higher than that calculated for the model $R\bar{3}c$ (curve c), whereas is more similar to that calculated for the model *R*3*c* (curve b).

The fractional coordinates of the atoms of the asymmetric unit of the model of Figure 11 for the space group $R\bar{3}c$, corresponding to the average position of the chain shown in Figures 10 and 11, are reported in Table 6. As discussed above, the coordinate corresponding to the disordered model that gives the best agreement of Figure 12 and Tables 4 and 5 can be obtained by introducing disorder in the rotations of the chains of about ±17° around the chain axes with respect to the average position.

The proposed models of crystal structure indicate that the presence of hexene comonomeric units in the crystals plays the most important role in the crystallization of the new form. The inclusion of hexene comonomeric units in the crystal lattice produces an increase of mass of about 25%, in the case of the sample iPPHe26, so that the mass of matter inside the hexagonal unit cell becomes as high as that of form I of iPB (Figure 7B). Therefore, if the volume of the hexagonal unit cell was similar to that of form I of iPB,[13] crystals of the iPPHe26 copolymer in the trigonal form would achieve a density as high as that of

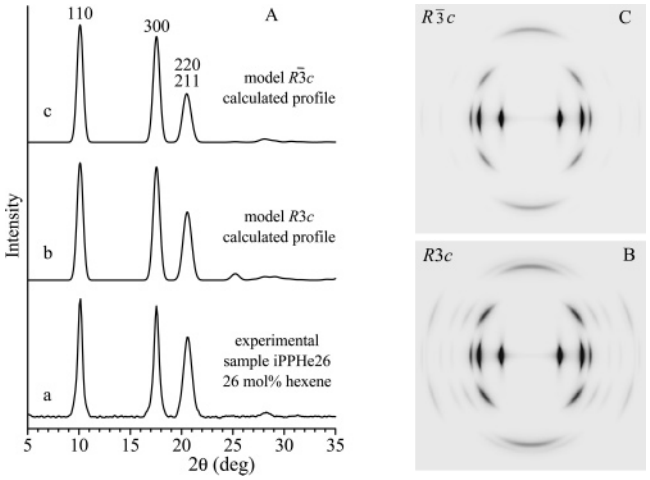

Figure 12. Experimental X-ray powder diffraction profile of the sample iPPHe26 with 26 mol % of hexene units, after the subtraction of the amorphous halo (A, curve a), calculated X-ray powder diffraction profiles (A) and calculated X-ray fiber diffraction patterns (B, C) for the disordered model of crystal structure of Figure 10 in the space group *R*3*c* (A, curve b and B) and for the limit disordered model of Figure 11 in the statistical space group *R*3̄*c* (A, curve c and C). Both models *R*3*c* and *R*3̄*c* present a slight disorder in the orientation of the chains around the chain axes corresponding to rotations of chains of ±17° around the chain axes with respect to the average positions of chains shown in the model of Figure 10. Moreover, in the model *R*3̄*c* (Figure 11) additional statistical disorder in the positioning of up and down 3-fold helices in each site of the lattice is present.

Table 6. Fractional Coordinates of the Asymmetric Unit in the Models of Figure 11 of the Crystal Structure of the Trigonal Form of Copolymers iPPHe in the Space Group *R*3*c*[a]

atom	*x*/*c*	*y*/*c*	*z*/*c*	occupancy factor
C1	0.288	0.288	−0.065	0.500
C2	0.288	0.288	0.170	0.500
C3	0.232	0.192	0.250	0.500
C4	0.136	0.143	0.170	0.125
C5	0.081	0.049	0.251	0.125
C6	−0.013	0.001	0.170	0.125
H1	0.318	0.249	−0.118	0.500
H2	0.220	0.254	−0.124	0.500
H3	0.252	0.321	0.222	0.500
H4	0.265	0.154	0.210	0.500
H5	0.227	0.191	0.419	0.500
H6	0.104	0.181	0.211	0.125
H7	0.134	0.138	0.001	0.125
H8	0.114	0.011	0.210	0.125
H9	0.079	0.050	0.421	0.125
H10	−0.048	0.036	0.211	0.125
H11	−0.014	−0.005	0.001	0.125
H12	−0.051	−0.066	0.233	0.125

[a] The atoms C1−C3 and H1−H5 correspond the propylene monomeric unit, whereas the atoms C4−C6 and H6−H12 correspond to the lateral propyl group of the hexene comonomeric unit, which is present with a concentration of 26 mol %.

form I of iPB, as actually found. This simple density argument justifies the observation that propylene−hexene copolymers crystallize in the new trigonal form when the hexene concentration achieves a value higher than 10 mol %.

As a matter of fact the experimental crystalline density of the trigonal form of the sample iPPHe26 is slightly lower than that of form I of iPB (0.949 g/cm^3),[13] probably because, although the amount of hexene units incorporated in crystals of the trigonal form is definitely higher than that included in crystals of α form that forms at low hexene concentration (Figure 7B), hexene units are not totally included in the crystals, but, as demonstrated in Figure 7B, they are reasonably partitioned between crystalline and amorphous phases. Moreover, the unit cell dimensions ($a = 17.5$ Å) are already very close to those of form I of iPB ($a = 17.7$ Å),[13] allowing accommodation of bulky side groups, but the trigonal unit cell is probably still able to include higher amount of hexene units, for higher hexene concentrations, with only small changes of the volume, approaching the density of form I of iPB.

However, the achieved value of density of 0.905 g/cm^3 is high enough to induce crystallization of the trigonal form. In fact this form also crystallizes in copolymer samples with lower hexene concentration (for instance the samples iPPHe11 and iPPHe18 with 11.2 and 18 mol % of hexene, Figures 1i, 4A and 8B,D).

The hexene units are therefore included in the crystals of propylene−hexene copolymers inducing a suitable increase of density that allows crystallization of 3-fold helical chains of iPP in the trigonal form, where the helical symmetry of the chains is maintained in the crystal lattice, as foreseen by principles of polymer crystallography.[18,19] This form does not crystallize, and it has never been observed so far for the iPP homopolymer because, in the absence of bulky side groups, it would have a too low density. The 3-fold helical chains of iPP are instead packed in a monoclinic unit cell, according to the space groups *C*2/*c* or *P*2$_1$/*c*, so that the local symmetry of the chain conformation is lost in the lattice, allowing for a denser packing ($\rho_c = 0.936$ g/cm^3).[8] The trigonal structure of propylene−hexene copolymers represents the fulfillment of the principles of polymer crystallography and provides a clear example of the principle of *entropy-density driven phase formation* that suggests that the packing of polymer molecules is mainly driven by density.[2]

It is worth noting that the crystal structure of Figures 10 and 11 for iPPHe copolymers and the principle of density (entropy)-driven phase formation suggest that copolymers of propylene with olefins different from hexene may crystallize in a similar trigonal form, the form I-type iPB crystal structure, when the crystal density and the average composition of the copolymer approach those of iPB, provided that the distribution of the comonomer is random. The crystallization of the trigonal form probably occurs at higher comonomer concentrations in the case of smaller comonomer as, for instance, pentene, and at lower comonomer concentrations in the case of bigger comonomers, as heptene. However, in samples of random propylene-octene copolymers, recently studied by Poon et al.,[20] the crystallization of the trigonal form has not been observed. These copolymers, indeed, crystallize basically in the α form of iPP up to 12−13 mol % of octene. This could be due to the fact that the packing of macromolecules is also regulated by energy (principle of close packing), besides by the entropy−density factor.[18,19] Even though incorporating octene comonomer units in the crystals would produce a suitable increase of density, the bigger octene units cannot be probably easily accommodated in the structure of Figure 10 at low cost of energy because the contact distances between atoms of neighboring copolymer chains would be too short, lower than the sum of the van der Waals radii of atoms.

It is also worth mentioning that the principle of entropy-driven phase formation is confirmed by the fact that the essential condition for the crystallization of the trigonal form in propylene-based copolymers is the random distribution of the comonomer. In fact, in samples of propylene−hexene copolymers prepared with a different catalyst, reported by Shin et al.,[21] showing melting temperatures higher than those of our samples, probably due to a less homogeneous comonomer distribution, the crystallization of the trigonal form was not observed.[21] In fact, samples reported by Shin et al.[21] have been prepared with

a completely different catalyst, consisting of $Cr(acac)_3$ supported on $MgCl_2$, and show melting temperatures of 166 °C for the iPP homopolymer, indicating high stereoregularity, and of 120 °C for a propylene−hexene copolymer with hexene content of 13 mol %, against the melting temperature of only 90 °C of our sample iPPHe9 containing only 9 mol % of hexene units (Table 1). This probably indicates that our samples, as well as the samples studied by Poon et al.,[1] have a more homogeneous comonomer distribution, whereas in the samples reported by Shin et al.[21] the hexene units are more segregated in portions of chains producing longer regular propylene sequences that tend to crystallize in the usual α form.

Conclusions

The crystal structure of a new polymorphic form of iPP (the trigonal form) that crystallizes in isotactic propylene−hexene random copolymers is presented. For low concentrations of hexene comonomeric units, up to nearly 10 mol %, iPPHe copolymers crystallize in the α form of iPP. The new polymorphic form crystallizes when the hexene concentration achieves values higher than 9−10 mol %. X-ray diffraction and density measurements have indicated that the hexene units are included in both the crystals of α form and of the new trigonal form. Hexene units are naturally partitioned between amorphous and crystalline phases of copolymers, but the crystallization of the new trigonal form for hexene concentration higher than 10 mol % allows incorporation in the crystals of amount of hexene units higher than that included in crystals of α form.

The melting temperature and the crystallinity of iPPHe copolymers decrease rapidly with increasing hexene content up to 7−8 mol %. Because of the crystallization of the new trigonal form a slower decrease of melting temperature and crystallinity is observed at higher hexene concentrations. This is in agreement with the hypothesis that hexene units are included in the crystals of α form for low concentrations and act as a lattice defect, producing large disturbance of the crystalline lattice and a consequent decrease of melting temperature, melting enthalpy and crystallinity. For concentrations higher than 7−8 mol %, larger amounts of hexene units are more easily accommodated in the crystalline lattice of the trigonal form producing a lower decrease of crystallinity and melting temperature.

The trigonal form does not crystallize from the melt of iPPHe copolymers but slowly crystallizes by aging amorphous samples at room temperature for about 24 h.

The crystal structure of the new form has been studied by analysis of X-ray powder and fiber diffraction patterns of samples containing hexene concentration higher than 9−10 mol %. Stretching of samples with high concentration of hexene (18 and 26 mol %), already crystallized in the new trigonal form, produces oriented fibers of the trigonal form, and a chain axis periodicity of 6.5 Å has been evaluated. Stretching of samples with lower hexene content (9 and 11.2 mol %) instead produces, as expected, formation of the mesomorphic form of iPP. Very surprisingly, the mesomorphic form transforms into the new trigonal form rather than into the α form, by annealing.

A model of the crystal structure of the trigonal form is proposed considering the diffraction data and the unit cell parameters of the sample with the highest concentration of hexene. Chains in 3-fold helical conformation of propylene−hexene copolymers are packed in a trigonal unit cell according to the space group $R3c$ or $R\bar{3}c$. The values of a and b axes of the unit cell increase with increasing hexene concentration, for instance values of $a = b = 17.5$ Å and $c = 6.5$ Å have been found for the sample with 26 mol % of hexene. The structure contains high degree of disorder due to the constitutional disorder of the random copolymer chains that produces disorder in the positioning of the lateral groups in the unit cell. Moreover, statistical disorder in the up−down positioning of the helical chains and slight disorder in the orientation of chains around the chain axes are present. The structure is similar to that of form I of isotactic polybutene. This form does not crystallize, and has never been observed so far for the polypropylene homopolymer because, in the absence of bulky side groups, it would have a too low density. The inclusion of hexene units in the crystals induces a suitable increase of density that allows crystallization of 3-fold helical chains in the trigonal form, where the helical symmetry of the chains is maintained in the crystal lattice. This trigonal structure represents the fulfillment of the principles of polymer crystallography and provides a clear example of the principle of *entropy−density driven phase formation* that suggests that the packing of polymer molecules is mainly driven by density.

Acknowledgment. Financial supports from Basell Polyolefins (Ferrara, Italy) and from the "Ministero dell'Istruzione, dell'Università e della Ricerca" of Italy (PRIN 2004 project) are gratefully acknowledged. We thank Davide Balboni for the synthesis of the copolymers, Isabella Camurati for the ^{13}C NMR analyses, and Oreste Tarallo for the X-ray diffraction analyses.

References and Notes

(1) Poon, B.; Rogunova, M.; Hiltner, A.; Baer, E.; Chum, S. P.; Galeski, A.; Piorkowska, E. *Macromolecules* **2005**, *38*, 1232.
(2) De Rosa, C.; Auriemma, F.; Corradini, P.; Tarallo, O.; Dello Iacono, S.; Ciaccia, E.; Resconi, L. *J. Am. Chem. Soc.* **2006**, *128*, 80.
(3) Lotz, B.; Ruan, J.; Thierry, A.; Alfonso, G. C.; Hiltner, A.; Baer, E.; Piorkowska, E.; Galeski, A. *Macromolecules*, submitted for publication.
(4) *Cerius*^{2} *Modeling Environment*; Molecular Simulations Inc.: San Diego, CA, 1999.
(5) Dinur, U.; Hagler, A. T. New Approaches to Empirical Force Fields In *Review of computational Chemistry*; 1991; Chapter 4. Maple, J. R.; Dinur, U.; Hagler, A. T. *Proc. Natl. Acad. Sci. U.S.A.* **1988**, *85*, 5350. Sun, H.; Mumby, S. J.; Maple, J. R.; Hagler, A. T. *J. Am. Chem. Soc.* **1994**, *116*, 2978. Sun, H. *Macromolecules* **1994**, *26*, 5942. Sun, H. *Macromolecules* **1995**, *28*, 701.
(6) Cromer, D. T.; Mann, J. B. *Acta Crystallogr.* **1968**, *A24*, 321.
(7) Turner Jones, A. *Makromol. Chem.* **1964**, *71*, 1.
(8) Natta, G.; Corradini, P. *Nuovo Cimento Suppl.* **1960**, *15*, 40.
(9) Brandrup, J.; Immergut, E. H.; Grulke, E. A. *Polymer Handbook*; John Wiley: New York, 1999.
(10) De Rosa, C.; Auriemma, F.; Di Capua, A.; Resconi, L.; Guidotti, S.; Camurati, I.; Nifant'ev, I. E.; Laishevtsev, I. P. *J. Am. Chem. Soc.* **2004**, *126*, 17040.
(11) De Rosa, C.; Auriemma, F.; De Lucia, G.; Resconi, L. *Polymer* **2005**, *46*, 9461.
(12) Alamo, R.; Domszy, R.; Mandelkern, L. *J. Phys. Chem.* **1984**, *88*, 6584.
(13) Natta, G.; Corradini, P.; Bassi, I. W. *Nuovo Cimento, Suppl.* **1960**, *15*, 52.
(14) Natta, G.; Corradini, P. *Makromol. Chem.* **1955**, *16*, 77.
(15) Corradini, P.; Bassi, I. W. *J. Polym. Sci., Part C* **1968**, *16*, 3233.
(16) Natta, G.; Corradini, P.; Bassi, I. W. *Nuovo Cimento, Suppl.* **1960**, *15*, 83.
(17) Natta, G.; Corradini, P. Bassi, I. W. *Rend. Fis. Accad. Lincei* **1957**, *23*, 363.
(18) Natta, G.; Corradini, P. *Nuovo Cimento, Suppl.* **1960**, *15*, 9. Natta, G.; Corradini, P. *J. Polym. Sci. Polym. Phys Ed.* **1959**, *29*, 29. Corradini, P. in *The Stereochemistry of Macromolecules*; Ketley, A. D., Ed.; Marcel Dekker: New York, Vol. 3, 1968; p 1.
(19) De Rosa, C. *Topic Stereochem.* **2003**, *24*, 71.
(20) Poon, B.; Rogunova, M.; Chum, S. P.; Hiltner, A.; Baer, E. *J. Polym. Sci., Polym. Phys.* **2004**, *42*, 4357.
(21) Shin, Y.-W.; Hashiguchi, H.; Terano, M.; Nitta, K. *J. Appl. Polym. Sci.* **2004**, *92*, 2949.

MA0606354